Electronic Supplementary Information

(1) Dielectric constant (ε′) and loss tangent (tanδ) for LGMO samples with x=0.05, x=0.1 and x=0.15, plotted as a function of frequency in the absence (H=0T) and presence of magnetic field (H=0.4T)

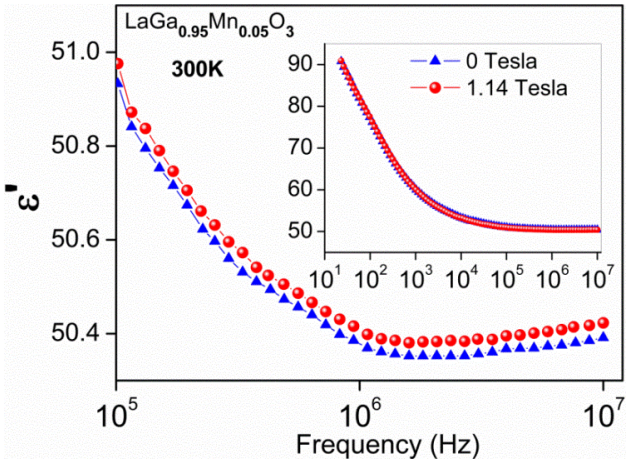

FIGURE-S1(a)

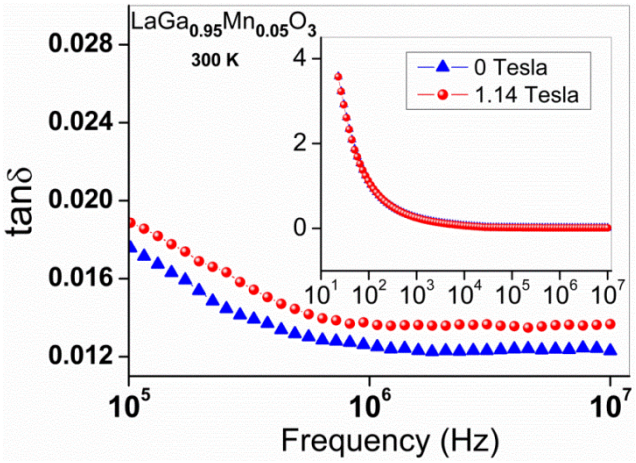

FIGURE-S1(b)

FIGURE-S1: Room-temperature (a) dielectric constant (ε′) and (b) loss tangent (tanδ) as a function of frequency measured in the absence (▲) and presence (●) of magnetic field for $LaGa_{0.95}Mn_{0.05}O_3$ (showing high frequency region i.e., from 100 kHz to 10 MHz). Inset shows the data for entire range of probing frequencies. It is clear from this figure that the change in RT ε′ is very little even in the presence of a high magnetic field of 1.14 Tesla. Both ε′ and tanδ are increasing with the application of magnetic field.

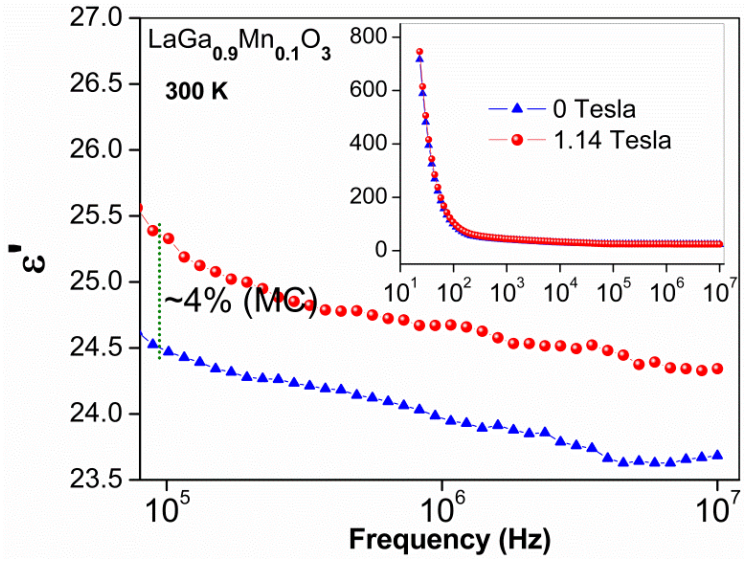

FIGURE-S2(a)

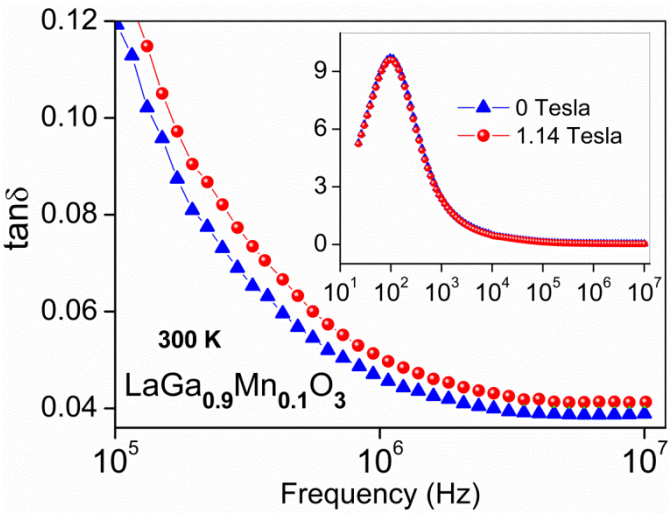

FIGURE-S2(b)

FIGURE-S2: Room-temperature (a) dielectric constant (ε′) and (b) loss tangent (tanδ) as a function of frequency measured in the absence (▲) and presence (●) of magnetic field for $LaGa_{0.9}Mn_{0.1}O_3$ (showing high frequency region i.e., from 100 kHz to 10 MHz). Inset shows the data for entire range of probing frequencies. A significant change of ~4% in RT ε′ is observed but with the application of a high magnetic field of 1.14 Tesla. A peak in tanδ is corresponding to a single dielectric relaxation. Both ε′ and tanδ are increasing with the application of magnetic field.

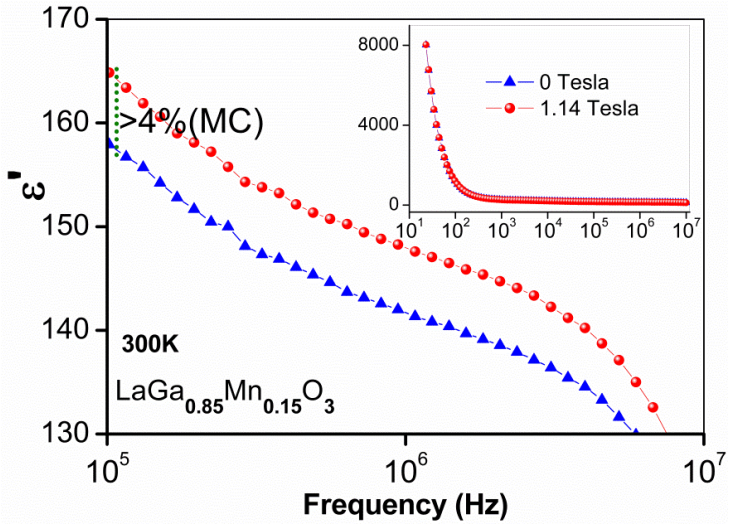

FIGURE-S3(a)

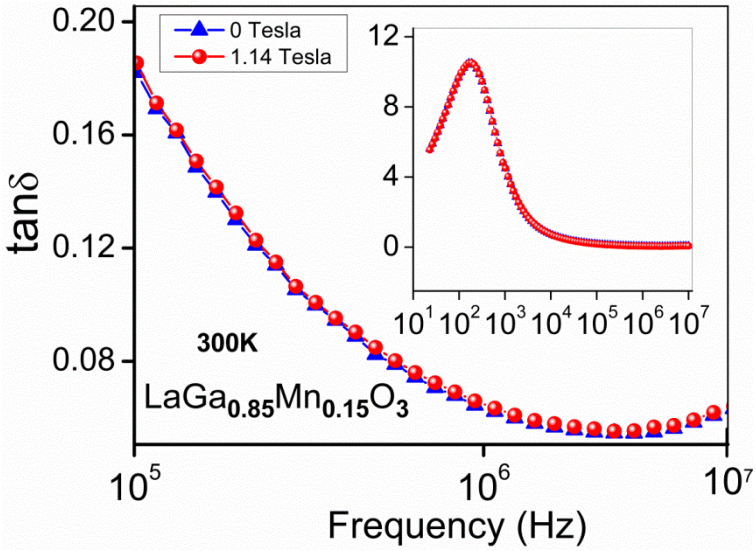

FIGURE-S3(b)

FIGURE-S3: Room-temperature (a) dielectric constant (ε′) and (b) loss tangent (tanδ) as a function of frequency measured in the absence (▲) and presence (●) of magnetic field for $LaGa_{0.85}Mn_{0.15}O_3$ (showing high frequency region i.e., from 100 kHz to 10 MHz). Inset shows the data for entire range of probing frequencies. A significant change of >4% in RT ε′ is observed but with the application of a high magnetic field of 1.14 Tesla. A peak in tanδ is corresponding to a single dielectric relaxation. Both ε′ and tanδ are increasing with the application of magnetic field.

Note- In figure S1 to S3, we have shown the percentage change in ε' due to the application of magnetic field as our major concerns are - MD effect and trend of change observed in ε′ and tanδ due to the application of magnetic field. Different values of ε' (~50 for x=0.05, ~25 for x=0.1 and ~160 for x=0.15) when measured at ~ 100 kHz, possibly, due to different Mn^{3+}/ Mn^{4+} ratios in LGO samples with different percentage of Mn doping or may have different origins that can be explored separately. But presently, our concern is the percentage change in ε′ (due to the application of magnetic field) and not its absolute value.

(2) Trends of change observed in MC% and ML% as a function of magnetic field for LGMO with x=0.2 (as a representative)

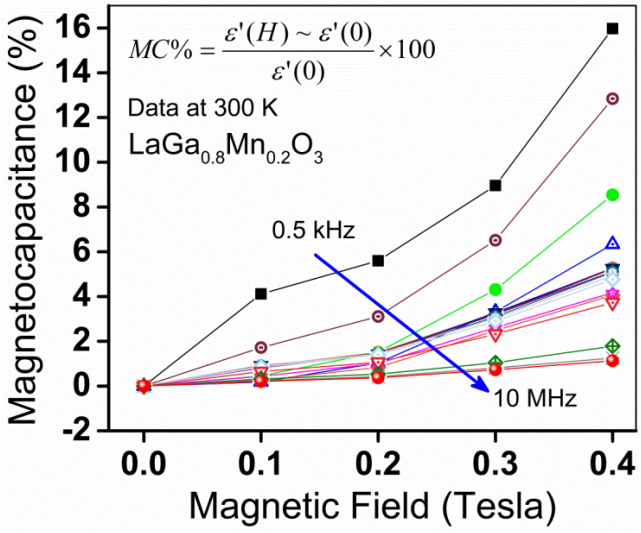

FIGURE-S4(a)

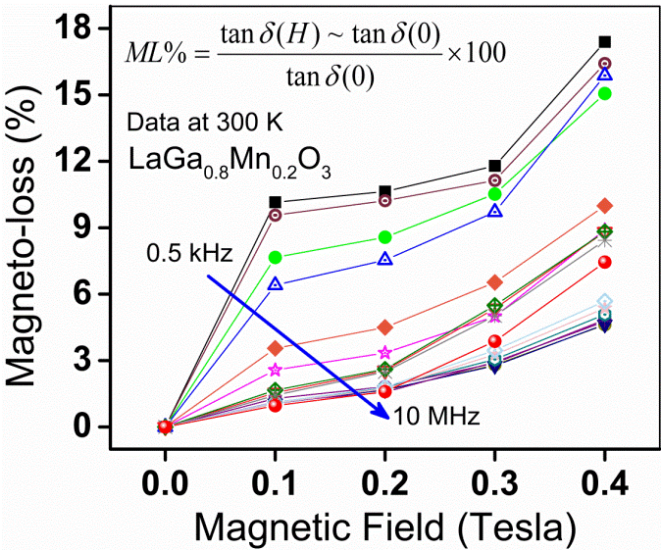

FIGURE-S4 (b)

FIGURE-S4: The trends of Room-temperature (RT) - (a) Magneto-capacitance (MC%) and (b) Magneto-loss (ML%) as a function of applied magnetic field for $LaGa_{0.8}Mn_{0.2}O_3$ measured at frequencies ranging from 0.5 kHz to 10 MHz. The observed trends (both MC% and ML% are increasing with magnetic fields for entire range of probing frequency) suggest that the presently appeared RTMD effect should be an intrinsic property of $LaGa_{0.8}Mn_{0.2}O_3$ as per the framework proposed by G. Catalan (Appl. Phys. Lett. **88**, 102902 (2006)) and also suggested by Mandal et al. (Phys. Rev. Lett. **107**, 137202 (2011)). Both MC% and ML% have been calculated by using the formulae shown in the corresponding figures. Where, ε′(0) and ε′(H) are the dielectric constant respectively in the absence and presence of magnetic field whereas tanδ(0) and tanδ(H) represent loss tangent respectively in the absence and presence of magnetic field.

(3) 'Mn^{3+}-Mn^{4+}' dipole; a pair of neighbouring $Mn^{3+}$and Mn^{4+} connected via oxygen ion

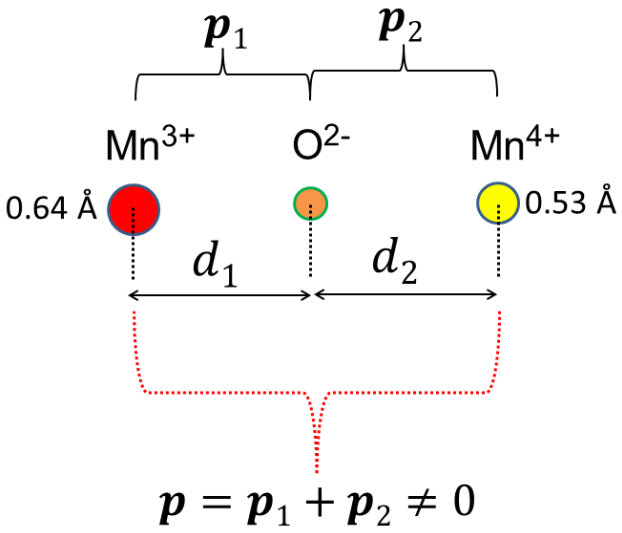

FIGURE-S5: Schematic presentation of a pair of neighbouring $Mn^{3+}$and Mn^{4+} connected via oxygen ion forming '$Mn3^{+}$-Mn^{4+}' dipole (net electric dipole moment **p**) as the chemical potential (charge) and ionic radii of $Mn^{3+}$and Mn^{4+} are different from each other.

(4) One of the possible distribution of 'Mn^{3+}-Mn^{4+}' dipoles in LGMO ($LaGa_{1-x}Mn_xO_3$) system

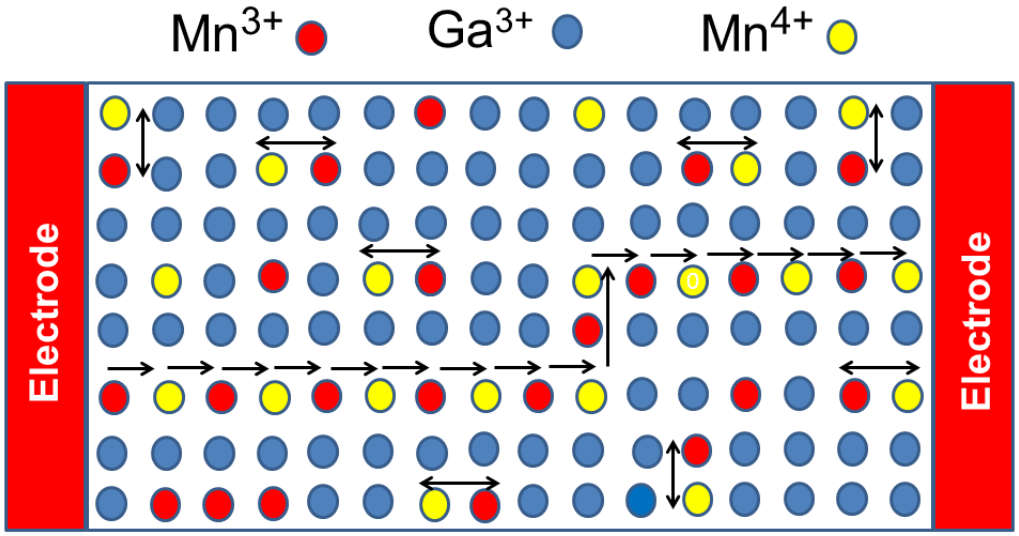

FIGURE-S6: Schematic representation of one of the possibility assumed for electron transport (through the material i.e., LGMO sample sandwiched between two electrodes in parallel plate capacitor geometry) between end electrodes by means of electron hoping via depicted Mn^{3+}-Mn^{4+}-Mn^{3+} …… route. The double head arrow is indicating a locally flipping pair of Mn^{3+} and Mn^{4+} whereas as single head arrow shows the direction of electron transport. For simplicity lanthanum and oxygen ions are not shown whereas Ga^{3+}, Mn^{3+} and Mn^{4+} ions are represented by blue, red and yellow balls respectively.

(5) dc MR (magneto resistance) at room temperature

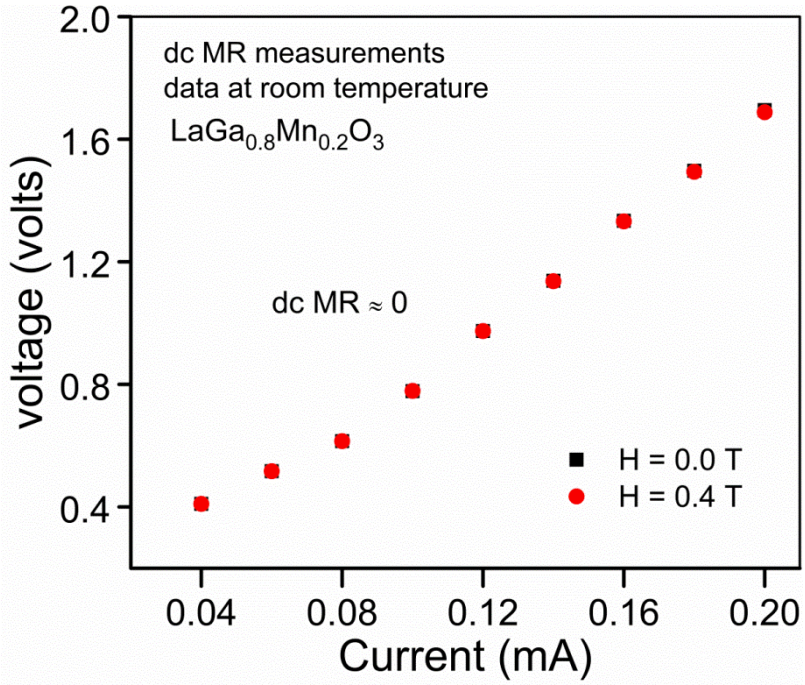

FIGURE-S7: Room temperature current-voltage (I-V) graph plotted by measuring the voltage for different currents in the absence (H=0 T ■) and presence (H=0.4 T ●) of magnetic field using the four-probe method. This MR data reveals that there is no negative dc MR is present in $LaGa_{0.8}Mn_{0.2}O_3$.

(6) Relation between dielectric permittivity, loss tangent and conductivity

It is well known that loss tangent (tanδ) plays important role in understanding the dielectric/MD properties. It (tanδ) can be expressed by following relation (derived from Maxwell's 4th equation of electromagnetism)

$$\tan\delta = \frac{\omega\varepsilon'' + \sigma}{\omega\varepsilon'} \qquad (1)$$

Here, ω is the frequency of applied electric field whereas ε″ is the imaginary component of permittivity attributed to bound charge and dipole relaxation phenomena (associated with the dipolar oscillations), which gives rise to energy loss. This energy loss is indistinguishable from the loss due to the free charge conduction quantified by σ. The component ε′ represents the lossless permittivity (dielectric constant) given by the product of the free space permittivity and the relative real permittivity, or $\varepsilon' = \varepsilon_0\varepsilon_r'$.

(7) Discussion on the correlation between pre-edge feature in XANES data and off-centro-symmetry around MnO_6 octahedron

It has been already reported by Joly et al.[1] that pre-K-edge features in $A(TM)O_3$ (TM:transition metal ion) oxides arise possibly due to the strong mixing of 3*d* states of neighboring TM atoms via hybridization with 2*p* states of intermediate oxygen which is supported well by other reports [2,3]. This strong mixing of 3*d* states probably causes local distortions which may lead to the reduction in symmetry around the TM atom in the $(TM)O_6$ octahedron [3] and consequently gives rise to a net electric dipole moment (polarization). It is noticeable that the intensity of pre-K-edge feature signifies stronger reduction in the cetrosymmetry of the $(TM)O_6$ octahedron i.e., it is a measure of strength of the above-mentioned mixing of 3*d* states via oxygen 2*p* states [3,4]. For the present LGMO system, the appearance of pre- K-edge feature may be credited to $1s \rightarrow 3d$ dipolar (forbidden) and quadrupole (allowed) transitions [2,3]. The contribution of the latter transitions is weaker whereas the former ones contribute strongly as they become allowed probably due to the above-discussed strong mixing of Mn 3*d* states via oxygen 2*p* states [1–3].

(8) Room temperature P-E measurements

The RT ferroelectric hysteresis i.e. P-E loop was recorded for all presently studied LGMO samples by using precision material analyzer (Radiant Technologies INC). The obtained P-E data is shown below in Figure S8.

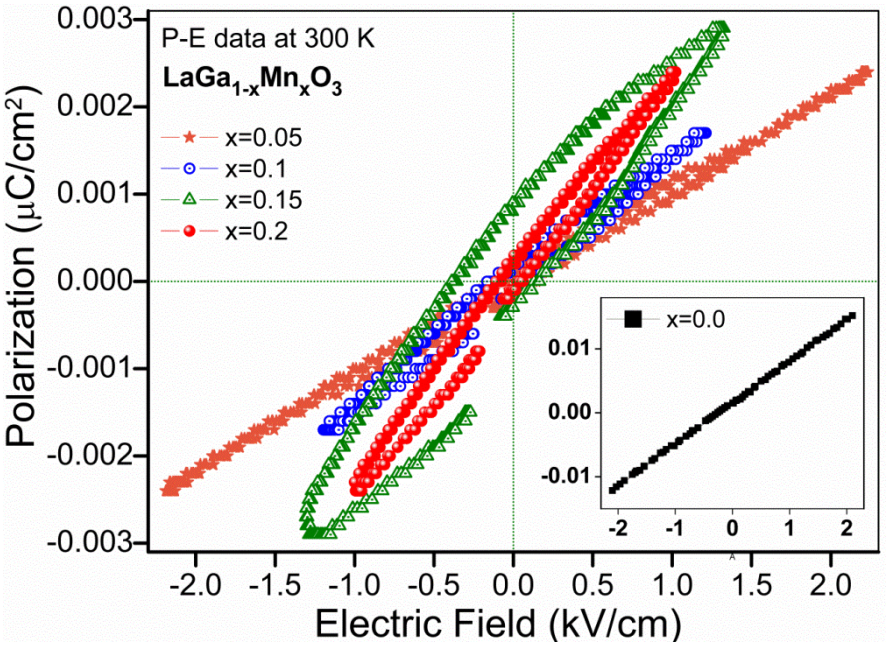

FIGURE-S8: Room temperature P–E plots for LGMO samples with x=0 to x=0.2. The data for LGMO sample with x=0.1 is shown separately in the inset as it is linear and not showing any opening in loop.

It is clear from inset of Figure S8 that, undoped LGO displays a linear dielectric behavior whereas all Mn doped LGO samples exhibit a RT hysteresis (P-E) loop (main panel). It is vital to note that the ferroelectric contribution (intrinsic polarization) is negligible as the shape of the observed P–E loops is similar to that appears due to leakage currents [5,6]. Conversely, the corresponding pre-K-edge feature (a signature of breaking of inversion symmetry around transition metal (TM)[7]), observed in the XANES data (Figure 6 of main text), points towards the possibility of a finite ferroelectric contribution associated with the breaking of inversion symmetry around TM [7] (Mn in present case). However, it is important to mention that similar RT P-E (even more leaky) and M-H loops observed for Ca doped (at Bi site) $BiFeO_3$ are reported as the signature of Multiferroicity [8]. Thus, low temperature (LT) P-E measurements (but only upto transition temperature of ferromagnetic ordering (T_{FM}) because below T_{FM} the ferromagnetic phase is generally supposed to be metallic) will be helpful in order to quantify a genuine polarization[9] in the presently studied LGMO samples as the leakage decreases at low temperatures i.e., for a semiconductor like LG8M2O, insulating behavior evolves with decreasing temperature. Further, at LT, it is expected for pairs of neighboring Mn^{3+} and Mn^{4+} ions to form a stable localized dipole (due to difference in their chemical potentials) as the RT electron hoping between Mn^{3+} and Mn^{4+} sites [5] is expected to be ceased at LT [10]. As a whole, since presently studied LG8M2O shows FM ordering below 36 K (Figure 8 and 9 of main text) and may exhibit ferroelectric ordering either at the same temperature i.e., type-II multiferroicity or at a higher temperature i.e., type-I multiferroicity (as below FM phase is generally mettalic), therefore, we predict the possibility of multiferroicity in this sample. Further, in order to comment strongly about the correlation between electric and magnetic orders for presently studied LGMO systems, temperature dependent P-E experiments and/or measurements of temperature dependent ε' in ZFC-FC mode (electric field) are required as the transition temperature related to ferromagnetic (T_{FM}) and ferroelectric (T_{FE}) orders will be the deciding factor to classify the presently studied LGMO sample either as type-II (T_M and T_E are same) [11] or type-I multiferroic ($T_E > T_M$)[11].

References

1 Y. Joly, D. Cabaret, H. Renevier and C. R. Natoli, *Phys. Rev. Lett.*, 1999, **82**, 2398–2401.
2 M. C. Sánchez, G. Subías, J. García and J. Blasco, *Phys. Rev. B*, 2004, **69**, 184415.
3 M. C. Sánchez, J. García, G. Subías and J. Blasco, *Phys. Rev. B*, 2006, **73**, 094416.
4 T. E. Westre, P. Kennepohl, J. G. DeWitt, B. Hedman, K. O. Hodgson and E. I. Solomon, *J. Am. Chem. Soc.*, 1997, **119**, 6297–6314.
5 H. M. Rai, S. K. Saxena, R. Late, V. Mishra, P. Rajput, A. Sagdeo, R. Kumar and P. R. Sagdeo, *RSC Adv.*, 2016, **6**, 26621–26629.
6 J. F. Scott, *J. Phys. Condens. Matter*, 2008, **20**, 021001.

7 F. J. Manjón, A. Segura, M. Amboage, J. Pellicer-Porres, J. F. Sánchez-Royo, J. P. Itié, A. M. Flank, P. Lagarde, A. Polian, V. v. Ursaki and I. M. Tiginyanu, *Phys. Status Solidi B*, 2007, **244**, 229–233.
8 D. Kothari, V. R. Reddy, A. Gupta, V. Sathe, A. Banerjee, S. M. Gupta and A. M. Awasthi, *Appl. Phys. Lett.*, 2007, **91**, 202505.
9 M. Shang, C. Zhang, T. Zhang, L. Yuan, L. Ge, H. Yuan and S. Feng, *Appl. Phys. Lett.*, 2013, **102**, 062903.
10 P. R. Sagdeo, S. Anwar and N. P. Lalla, *Phys. Rev. B*, 2006, **74**, 214118.
11 D. Khomskii, *Physics*, 2009, **2**, 20.